Journal of the Taiwan Institute of Chemical Engineers 108 (2020) 43–54

Contents lists available at ScienceDirect

Journal of the Taiwan Institute of Chemical Engineers

journal homepage: www.elsevier.com/locate/jtice

Investigation into an energy-saving mechanism for advanced stripper configurations in post-combustion carbon capture

Jialin Liu

Department of Chemical and Materials Engineering, Tunghai University, No. 1727, Sec.4, Taiwan Boulevard, Taichung, Taiwan, Republic of China

ARTICLE INFO

Article History:
Received 1 September 2019
Revised 12 December 2019
Accepted 30 December 2019
Available online 15 January 2020

Keywords:
Advanced stripper configurations
Energy savings
Post-combustion carbon capture
Regeneration process

ABSTRACT

In a standard post-combustion carbon capture (PCC) process, the regeneration energy of CO_2 lean solvent constitutes the majority of overall energy consumption. The energy reduction achieved by advanced stripper configurations, such as the cold-split bypass (CSB), interheated (IH) stripper, and lean vapor compression (LVC), have been reported in relevant literature. Energy-saving performance may be enhanced by combining the different modifications. In this study, the energy-saving mechanism for advanced stripper configurations was investigated using a standard amine-based process, in which 30 wt% monoethanolamine (MEA) aqueous solution was applied. Contrary to the literature reviewed, the energy-saving performance attained by combining the different modifications was limited. This was due to the major contribution of energy reduction in the various modifications sharing the similar mechanism. In addition, this study demonstrated that the overall energy required, as needed by the heat recovery in the cross-flow heat exchanger (HX) and the reboiler duty, is dominated by overhead vapor generation. Reducing the amount of vapor generated may effectively relieve the overall energy burden. Thus, when energy reduction is reliant on a HX with a poor heat recovery system, the energy-saving purpose is not fulfilled. Therefore, a successful energy-saving design may significantly reduce the amount of vapor generated, whilst maintaining a reliable heat recovery.

1. Introduction

Increasing amounts of CO_2 in the atmosphere from burning of fossil fuels contributes greatly to global warming. Recently, there has been substantial development in chemical absorption technology using amine-based absorbents for post-combustion CO_2 capture (PCC). The process of CO_2 capture using 30 wt% monoethanolamine (MEA) aqueous solutions is commercialized and is regarded as a standard for evaluating overall CO_2 capture performance. However, the MEA system endures a high regeneration energy penalty. Energy reduction in the stripper can be achieved by either formulating new solvents or optimizing the process configurations. Rochelle [1] compared the economics of PCC on a 450 MW power plant in 2001 and 2006, and reported that the regeneration energy was 0.51 and 0.37 megawatt-hours per metric ton of CO_2 (MWh/t-CO_2), respectively. This is around 5.2 and 3.7 GJ/t-CO_2 estimated at a 35.6% average generation efficiency [2]. The author indicated [1] that the contributions to energy reduction were due to solvent improvement and enhanced energy integration. However, the author declared that the solvent and process improvements were not substantially effective for energy reduction and that an energy consumption of less than 0.20 MWh/t-CO_2 (2.0 GJ/t-CO_2) should not be expected.

Typically, the heat requirement of a CO_2 stripper is determined by three major factors: CO_2 desorption energy, sensible heat of the rich solvent, and vaporization heat of the lean solvent. The regeneration heat is constituted mainly of desorption energy that breaks the CO_2-absorbent bonding, which is equivalent to the released heat as the CO_2 is absorbed by the lean solvent in the absorber. Mathonat et al. [3] used flow calorimetry to measure enthalpy changes in CO_2 absorption using a 30 wt% MEA aqueous solution at three temperatures (40, 80, and 120 °C) and three pressures (20, 50, and 100 bar), respectively. They reported that the heat released by absorption was determined by the reaction temperature and was independent of the pressure changes. The reported absorption enthalpies were 81, 90, and 102 kJ/mol-CO_2, which corresponded with 1.84, 2.05, and 2.32 GJ/t-CO_2 at temperatures of 40, 80, and 120 °C, respectively. In addition, Kim and Svendsen [4] used a two-liter reaction calorimeter to measure the enthalpy of CO_2 absorption with a 30 wt% MEA solution. The experiments were conducted isothermally at temperatures ranging between 40–120 °C, and the CO_2 was pressurized at 2.8 – 3.0 bar. The results at 40, 80, and 120 °C corresponded with the enthalpy values measured by Mathonat et al. [3]. Therefore, the minimum CO_2 desorption energy should be in the range of 1.84–2.32 GJ/t-CO_2 and is dependent on the desorption temperature.

E-mail address: jialin@thu.edu.tw

https://doi.org/10.1016/j.jtice.2019.12.012

Other than bench-scale tests, Notz et al. [5] installed a pilot plant in which the closed cycle of CO_2 absorption/desorption could be continuously operated using a 30 wt% MEA solution. The plant was equipped with columns 0.125 m in diameter, absorber/desorber packing heights of 4.2/2.5 m, and the packing type was Sulzer Mellapak 250.Y^{TM}. Controlled factors included the flow rate of flue gas at 30–110 kg/h, CO_2 partial pressure at 35–135 mbar, solvent flow rate at 50–350 kg/h, and CO_2 lean loading at 0.111–0.356 mol-CO_2/mol-MEA. The results showed that the CO_2 removal rate reached 40.3–91.2% and the energy required was approximately 3.68–10.24 GJ/t-CO_2, of which the desorption energy constituted 2.26–2.45 GJ/t-CO_2. Notz et al. [5] concluded that the specific energy requirement for the desorption of CO_2 was aligned with the absorption heat of 30 wt% MEA aqueous solution, which is almost independent of the controlled factors. Subsequent work conducted by Mangalapally and Hasse [6] using the same equipment (only the packing type was different, namely, Sulzer BX 500), found that the CO_2 lean loading varied from 0.041 to 0.308 mol-CO_2/mol-MEA, and that the CO_2 removal rate could reach 40.3–91.2%. The energy requirement ranged from 3.23 to 10.31 GJ/t-CO_2, with the desorption energy using 2.21–2.43 GJ/t-CO_2. Results of the pilot-plant tests [5,6] were consistent; the minimum requirement for desorption energy was 2.21–2.45 GJ/t-CO_2 by 30 wt% MEA solution. In addition, the results [6] showed that the regeneration energy required was around 3.57–4.72 GJ/t-CO_2 to achieve a 90% CO_2 removal rate, where the lean loading was in a range of 0.20–0.27 mol-CO_2/mol-MEA.

A pilot plant campaign, which consisted of 48 runs at 24 different operating conditions, was carried out by Dugas [7]. Two identical columns were equipped with one as the absorber and the other as the stripper. The diameters and total packing heights of the columns were 0.427 and 6.10 m, respectively. Two types of packings, Flexipac 1Y and IMTP no. 40, were tested, and the experimental conditions were as follows: the flue gas rate was 5.50–13.75 m^3/min with a CO_2 inlet of 15.2–18.0 mol%, a lean solvent rate of 13.2–104.1 L/min, and a CO_2 lean loading range of 0.15–0.37 mol-CO_2/mol-MEA. The CO_2 removal rate was between 61% and 99%. Based on the pilot-plant data, Zhang et al. [8] developed a rate-based absorption model using the Aspen Plus process simulator. The mass transfer coefficients and interfacial area for the random packing (IMTP no. 40) were estimated using correlations with research conducted by Onda et al. [9]. Similarities with the study by Stichlmair et al. [10] were used to predict the liquid holdup. For the structured packing type of Flexipac 1Y, the mass transfer coefficients and liquid holdup were calculated using correlations with Fair and Bravo [11] and Bravo et al. [12], respectively. To determine the reaction kinetics, reaction constants for the forward reactions of carbamate and bicarbonate formations were regressed using data from Aboudheir [13]; and reaction constants for the reverse reactions were calculated using the chemical equilibrium constants and corresponding constants for the forward reactions. Zhang et al. [8] evaluated the prediction performance of four combinations of equilibrium/rate-based models and equilibrium/kinetic reactions with the pilot-plant data [7]. They concluded that the data could be described by the absorption model if the rate-based and kinetic models were considered simultaneously. Other combinations could overestimate the CO_2 rich loading and the CO_2 removal rate. In addition, the types of film resistance (ignore film, consider film, film reactions, and discretize film reactions) were evaluated using the absorber temperature profiles from the pilot-plant data. They reported that the temperature profiles could be determined using the liquid film discretization option. The discretization number may not affect the predicted performance. The mass transfer and reaction rates in the liquid and vapor films were evaluated using the interface properties and the respective bulk phase. The option of flow model such as Mixed, CounterCurrent, Vplug, or Vplug-Pavg needs to be predetermined for calculating the properties of the bulk phases. Zhang et al. [8] reported that the flow models have a minor impact on the prediction of absorber temperature profiles with the Mixed model resulting in the most reliable predictions.

Lin et al. [14] applied the rate-based model developed by Zhang et al. [8] to modify the traditional stripper configuration and to reduce the reboiler duty. Three types of modification were considered, namely, cold-split bypass (CSB), interheated (IH), and a combination of CSB and IH. The simulation settings for their base case [14] included: 9 m (mol/kg H_2O) MEA solution, CO_2 lean loading of 0.40 mol-CO_2/mol-MEA, and a stripper pressure of 3.3 bar. The reboiler duty of the simple stripper was reported as 145.6 kJ/mol-CO_2 (3.31 GJ/t-CO_2). For CSB, a 5.8% energy reduction (in comparison with the base case) could be achieved. The partial latent heat of the overhead vapor fed directly into the condenser was recovered by the CSB flow. In addition, the IH stripper could save around 8.0% of reboiler duty, in comparison with the base case. The semi-lean solvent was drawn from the middle of the stripper and heated by the hot lean solvent from the bottom by the interheater; the heated semi-lean solvent was then sent back to the next stage. Because the partial sensible heat of the hot lean solvent was recovered by the interheater, the temperature of the warm-rich solvent fed into the stripper was lower than that of the simple stripper. Energy savings stemmed from condensing the steam in the stripper, this is a similar process to the CSB configuration but it occurs at a higher temperature. Thus, the CSB flow was fed into the top of the IH stripper to recover the vapor heat. The combination of CSB and IH was reported to achieve an energy reduction 10.2% greater than the base case. In the work by Lin et al. [14] the energy-saving performance of the combined configurations exceeded that of each original modification; in addition, the energy reduction of the IH stripper outperformed that of the CSB configuration.

Le Moullec et al. [15] reviewed available literature as well as the patent database and summarized 20 elementary modifications to save energy during PCC. These methods can be categorized into three groups: absorption enhancement, heat integration, and heat pump. The energy-saving concept of absorption enhancement is to increase the rich loading at the absorber bottom. In the case of a constant removal rate e.g., 90%, lower amounts of lean solvent are needed to reduce the sensible heat of the rich solvent. The general principle of heat integration for energy saving is to reduce heat loss by modifying the process e.g., the CSB recovers heat from overhead vapor that was fed directly into the condenser. Thereby, a reduction of 10–12% in reboiler duty could be achieved using the CSB configuration. In addition, they reported a 13.4% reduction in reboiler duty using an IH stripper, which optimizes the temperature profile by integrating hot lean solvent from the reboiler. Karimi et al. [16] indicated that for effective desorbing of CO_2 it is important to maintain a high temperature at the bottom of the stripper. Additionally, maintaining a low temperature at the top of the stripper is important for increasing the CO_2/H_2O partial pressure ratio. However, according to the survey by Le Moullec et al. [15], 39.0% of energy savings were reportedly due to integrating CSB with an IH stripper. Also, the modification of the heat pump increases the heat quality at the cost of additional shaft work. For example, in the lean vapor compression (LVC) configuration, the hot lean solvent was flashed to produce a gaseous stream. The vapor was then compressed and fed back into the stripper. This relieves the reboiler duty as the compressed vapor and the flashed liquid possess lower temperatures thereby allowing for the temperature of the warm-rich solvent to decrease after the main cross-flow heat exchanger (HX). The LVC loss reduction ranges from 1.4–11.6%, as reported by Le Moullec et al. [15]. This loss reduction was further enhanced to 8.4–16.9% by combining LVC with CSB modifications.

The minimum regeneration energy achieved with 30 wt% MEA solution was 1.67 GJ/t-CO_2, as reported in the work of Higgins and Liu [17]. The energy consumption of their base case was 4.10 GJ/t-CO_2 at a stripper pressure of 1.4 bar and a lean loading of 0.18 CO_2. After a series of process modifications that included (i) absorber

intercooling, (ii) stripper interheating, (iii) multipressure stripping, (iv) vapor recompression, (v) distributed cross heat exchanger, and (vi) stripper condensate redirection, the regeneration energy could be reduced to 2.86 GJ/t-CO_2, which achieved an energy reduction of 30.2% in comparison with their base case. With the integration of an absorption-driven heat pump into the PCC process, waste heat (at a temperature higher than 58.9 °C) was recovered from the absorber and stripper condensers by the working flow (aqueous lithium bromide, LiBr). To raise the waste heat temperature, the heat pump needs a high temperature steam (236 °C and 31.2 bar) to vaporize the working flow. To recover 0.329 MW of waste heat, 0.465 MW of high quality steam is required i.e., the waste heat only uses 41.4% of the heat source provided by the heat pump and the remaining 58.6% is obtained from the steam. Because the traditional stripper is heated by low-pressure steam, the heat pump approach may not be cost-effective if the price of high-pressure steam is 1.7 times that of low-pressure steam.

The survey results [15] and simulations [14,17] suggest that the energy-saving achieved by combining different schemes is superior to individual performance e.g., the energy reduction of integrating CSB with IH is better than that of CSB or IH alone. However, when the advanced stripper configurations possess the same energy saving mechanism, combining them may not result in a substantial performance enhancement. In this study, the energy-saving effect of the various stripper configurations is investigated using Aspen Plus V10. The following sections of this paper are organized as follows: Section 2 provides validation for the simulation model with the pilot-plant data [5], Section 3 provides the baseline for standard amine-based PCC as per the results of Ahn et al. [18], Section 4 presents the investigation into energy savings by the advanced stripper configurations, and finally, the conclusions are presented in Section 5.

2. Model validation

The Redlich-Kwong equation of state and the electrolyte-NRTL method were used to compute the properties of the vapor and liquid phases, respectively. In addition, all the ionic reactions can be assumed to be in equilibrium, as listed in (R1)-(R3), where the equilibrium constants are calculated from the Gibbs free energy change.

$$MEAH^+ + H_2O \leftrightarrow MEA + H_3O^+ \quad (R1)$$

$$2H_2O \leftrightarrow H_3O^+ + OH^- \quad (R2)$$

$$HCO_3^- + H_2O \leftrightarrow CO_3^{-2} + H_3O^+ \quad (R3)$$

In the rate-based model, the rate-controlled reactions of CO_2 with OH^- and MEA are concerned as following:

$$CO_2 + OH^- \rightarrow HCO_3^- \quad (R4)$$

$$HCO_3^- \rightarrow CO_2 + OH^- \quad (R5)$$

$$MEA + CO_2 + H_2O \rightarrow MEACOO^- + H_3O^+ \quad (R6)$$

$$MEACOO^- + H_3O^+ \rightarrow MEA + CO_2 + H_2O \quad (R7)$$

where the reaction rate is described by the reduced power law:

$$r = k\exp\left(\frac{-E}{RT}\right)\prod_{j=1}^{N}\left(x_j\gamma_j\right)^{a_j} \quad (1)$$

In Eq. (1), the concentration basis is expressed as mole gamma where x_j, γ_j and a_j are the mole fraction, the activity coefficient and the stoichiometric coefficient of component j; the rate constants of k and E are listed in Table 1. It should be noted that two sets of rate constants are provided by the technical document [19]. One is approximated by a reaction temperature between 30 and 80 °C, which is the range at which the absorber operates; and, the other is for simulating the stripper where the temperature ranges between 80 and 120 °C. The parameter settings for the rate-based model can also be found in the technical document [19]. The simulation model was validated by data obtained from Notz et al. [5] where the diameter of absorber and stripper was 0.125 m, the packing heights of absorber and stripper were 4.20 m and 2.52 m, respectively, and the structured packing Flexipac 250Y was applied. The mass transfer coefficients and liquid holdup were calculated using correlations with Fair and Bravo [11] and Stichlmair et al. [10], respectively. Since CO_2 absorption is diffusion-controlled, the absorber was simulated using the rate-based model. The reaction condition factor was adjusted to 0.9, and the VPlug flow model was used. The vapor film resistance had been concerned, and the liquid film was discretized into six regions, which the number of discretization points was set as five. Fig. 1(a) shows the errors between the simulation results and the pilot-plant data for CO_2 removal rates, which are within ±15%. This suggests that the simulation model can describe the behavior of CO_2 absorption using 30 wt% MEA solution. However, due to the high temperature in the stripper, the CO_2 desorbed from the carbamate and bicarbonate may not be limited by the diffusion rate. Fig. 1 (b) compares the simulation results of the stripper, using the rate-based and equilibrium models, with the experimental data [5] for regeneration energy (the errors for both models are within ±15%). In addition, Fig. 1(c) compares the simulation results for the equilibrium model with the experimental data [5] for the reboiler temperature, in which the errors fall within ±3%. The rate-based and equilibrium models can be used to describe the energy consumption of the stripper and the reboiler temperature can be presented using the equilibrium model. This study used the equilibrium model to simulate the stripper operation due to its simplicity with regards to numerical convergence.

Table 1
Parameters k and E in Eq. (1) [19].

Reaction No.	k (kmol·m^{-3}·s^{-1})	E (cal·mol^{-1})
R4	1.33×10^{17}	13,249
R5	6.63×10^{16}	25,656
R6	3.02×10^{14}	9855.8
R7 (Absorber)	5.52×10^{23}	16,518
R7 (Stripper)	6.50×10^{27}	22,782

3. Standard process

A standard 30 wt% aqueous MEA solvent was used to capture 90% of CO_2 from the flue gas of an exemplary 550 MW coal-fired power plant [18]. The mass flow rate of the flue gas was 2067 metric ton/h at 43.6 °C and 1.3 atm. The flue gas composition was 4.06% H_2O, 2.20% O_2, 78.09% N_2, and 15.65% CO_2 by volume. Fig. 2 shows a conventional amine-based PCC process configuration. The flue gas was fed into the bottom of the absorber where the cold lean solvent was trimmed to 45 °C (Ahn et al., 2013) and then was fed into the column from the top to capture 90% of the CO_2. The CO_2 rich solvent was used to recover the sensible heat of the hot lean solvent in the cross-flow heat exchanger (HX), in which the minimum temperature approach was set as 5 °C. Next, the warm rich solvent was fed into the stripper from the top and the overhead vapor condensed at 40 °C. Ahn et al. [18] reported that the estimated energy consumption by the stripper was around 3.5 GJ/t-CO_2 when the stripper pressure was set at 1.9 atm and a lean loading of 0.23 was applied. The absorber was packed with Flexipac 250Y. The column sizes were not provided by Ahn et al. [18]. In this study, the column diameter was determined by calculating 80% of the maximum flood capacity and the packed height was estimated using a rich solvent loading of 0.49 [18]. The column diameter and packed height for the absorber were 18 m and 15 m, respectively.

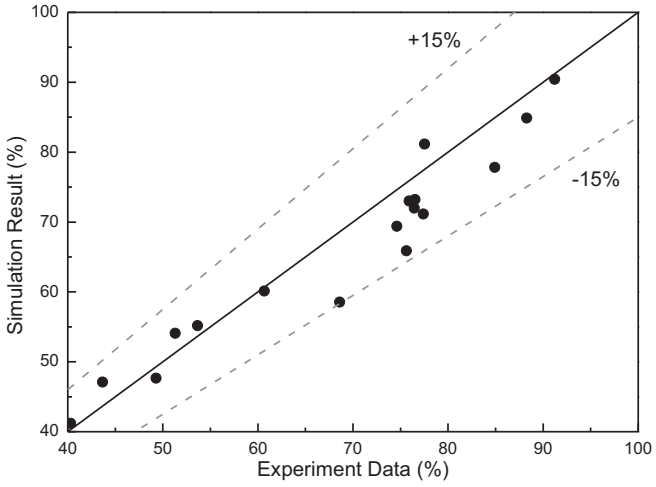

(a)

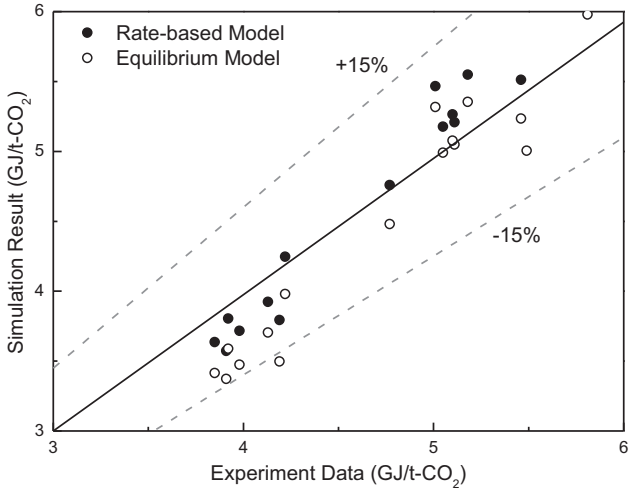

(b)

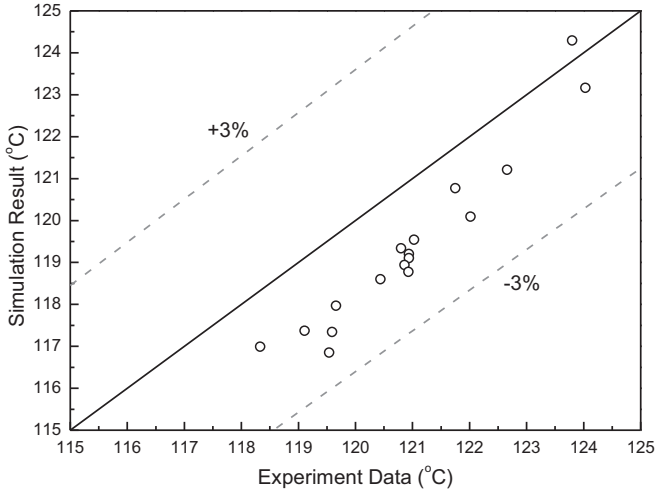

(c)

Fig. 1. Simulation model validations, where (a) CO_2 removal rate, (b) regeneration energy, and (c) reboiler temperature.

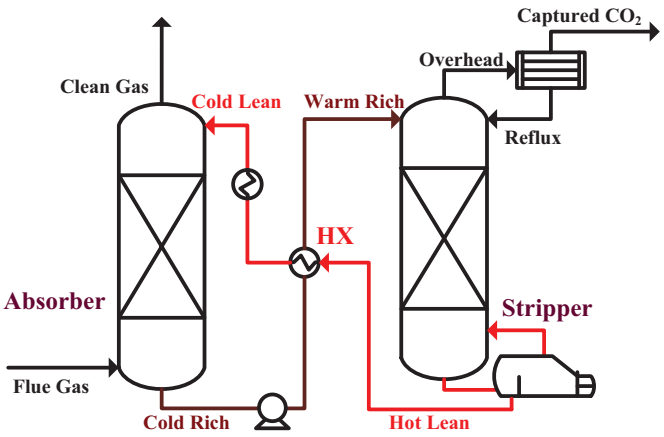

Fig. 2. Process flow diagram of amine-based PCC.

With a targeted 90% CO_2 removal rate, the solvent requirements are proportional to the CO_2 lean loading, as shown in Fig. 3. Fig. 4(a) illustrates that the regeneration energy is proportional to the required amount of lean solvent, in which 20 equilibrium stages [19] were applied to simulate the stripper, as increasing the CO_2 lean loading. On the other hand, the regeneration energy is also increasing at lower loadings. For example, the minimum regeneration energy is around 3.4 GJ/t-CO_2, at a lean loading of 0.18 and a pressure of 3 atm. In addition, as shown in Fig. 4(a), the regeneration energy was around 3.6 GJ/t-CO_2, at a lean loading of 0.23 and a pressure of 2 atm, which was similar to the result of 3.5 GJ/t-CO_2 obtained by Ahn et al. [18]. Fig. 4(a) also shows that energy consumption can be reduced by increasing the stripper pressure. Because CO_2 desorption is an endothermic reaction, high temperatures in the column encourage CO_2 to be desorbed from the carbamate and bicarbonate. However, thermal degradation of the MEA solvent is accelerated when the reboiler temperature is above 135 °C [20]. Therefore, due to the temperature limitation, the advanced stripper configurations were investigated using a pressure of 3 atm and a lean loading above 0.2, as shown in Fig. 4(b).

4. Advanced stripper configurations

In this study, the energy-saving mechanism for three types of advanced stripper configurations, namely, CSB, IH, and LVC, were

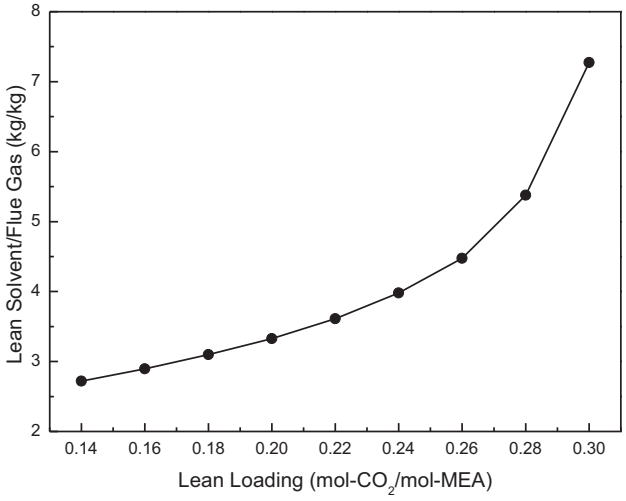

Fig. 3. The mass flow ratio of required lean solvent to flue gas.

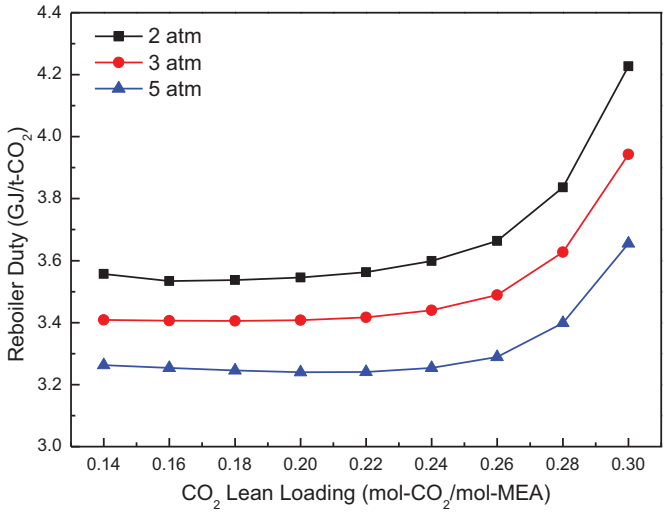

Fig. 4. Results for regenerating the MEA solvent, where (a) reboiler duty, and (b) reboiler temperature.

investigated. In the review paper [15], the authors reported that the reductions in reboiler duty obtained were 10–12% and 13.4% for the CSB and IH processes, respectively, and that the parasitic loss could be reduced to 1.4–11.6% for the LVC configuration. However, the reduction of reboiler duty by combining the CSB and IH can be enhanced further to 39.0% and the reduction in parasitic loss by combining the LVC and CSB can be improved to 8.4–16.9%. The significant energy savings and parasitic loss reductions by integrating advanced stripper configurations inspired this research to investigate the respective energy-saving mechanisms.

4.1. Cold-split bypass

Fig. 5 shows the process flow diagram for CSB, where a fraction of the cold-rich solvent was separated and fed into the top of the CO_2 stripper with the remaining cold-rich solvent used to recover the sensible heat of the hot lean solvent. The warm-rich solvent was fed into the stripper at a lower location than that of the cold-rich solvent. The feed stage of the warm-rich solvent may affect the energy consumption of the CSB process. Fig. 6 shows the results obtained by varying the warm-rich feed stage and the cold-split fraction at a CO_2

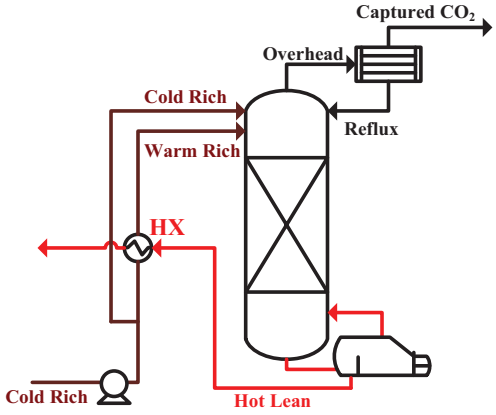

Fig. 5. The process flow diagram of CSB.

lean loading of 0.22. As shown in Fig. 6(a), once the feed stage of the warm-rich solvent was maintained at the top, the reboiler duty increased with the increasing cold-split fraction (the dashed line represents the energy requirement for a standard stripper). The more cold-rich solvent that was bypassed and directly fed into the top of stripper, the less sensible heat from the hot lean solvent was recovered; the deficiency was provided by the reboiler duty. On the other hand, as the warm-rich feed stage moved downward at a fixed cold-split fraction, the energy required reduced until a constant value was reached. In addition, Fig. 6(a) shows that the required energy decreased with an increase in the cold-split fraction until the minimum energy was reached at a cold-split fraction of 0.21. As depicted by the solid lines in Fig. 6(b), the top temperature of the stripper decreased as the warm-rich feed stage moved downward at each cold-split fraction, until the effect of the warm-rich feed stage was no longer evident. Therefore, the CO_2 purity at the top, which is the overhead flow in Fig. 5, increased due to the lowered temperature as shown by the dashed lines Fig. 6(b). With a constant CO_2 removal rate, the higher CO_2 purity in the overhead flow leads to a lower need for vaporization by the reboiler. Fig. 6(c) shows the vaporized ratio of overhead flow to the captured CO_2. Comparing Figs. 6(a) and 6(c), the reboiler duty is reduced due to a lower vaporized ratio and an increase in the cold-split fraction. When the CO_2 purity approaches one, the reduction of the vaporized ratio is limited by increasing the amounts of cold-split bypass. On the other hand, increasing the CSB flow results in poor heat recovery from the hot lean solvent. The deficiency in heat recovery is made up by the reboiler duty; therefore, at a cold-split fraction of 0.21, rather than 0.25, the minimum regeneration energy occurs at a lean loading of 0.22.

Fig. 7 summarizes the vaporized ratio of overhead flow to the captured CO_2 on varying the cold-split fraction at a CO_2 lean loading of 0.22, where the warm-rich feed stage was moved downward until the top temperature remained unchanged. The overall heat duty, which includes the duty recovered by the HX in Fig. 5 as well as the reboiler duty, decreases with a decreasing vaporized ratio, as shown in Fig. 7. The results in Fig. 7 demonstrate that the overall heat duty was mainly due to the amounts of vaporized overhead flow. In the cases of low bypass fractions, such as 0.05 and 0.07, the recovered heat duty by HX was not affected by the minor CSB flow rates. Therefore, the reduction in overall heat duty by lowering the vaporized ratio was contributed to the reboiler duty. In the case of large amounts of CSB flow e.g., cold-split fractions of 0.25 and 0.27, the vaporized ratio remained almost unchanged and the overall heat duty stayed constant. However, less sensible heat was recovered by the HX when the cold-split fraction increased from 0.25 to 0.27. When the overall heat duty remained unchanged despite increasing the cold-split fraction, the shortage of recovered duty needed to be compensated for by increasing the reboiler duty. Therefore, between

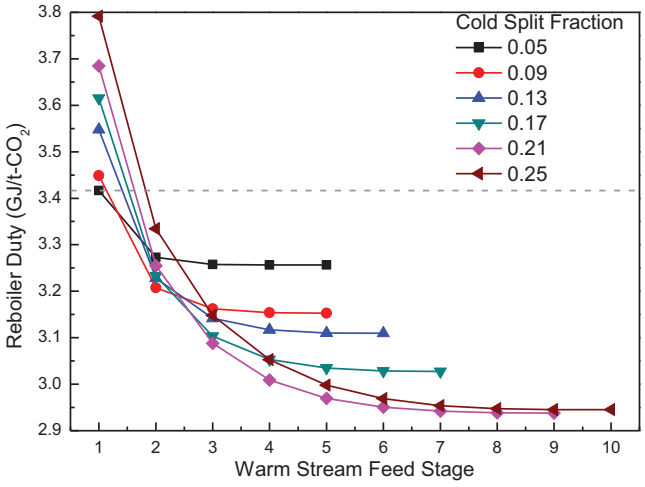

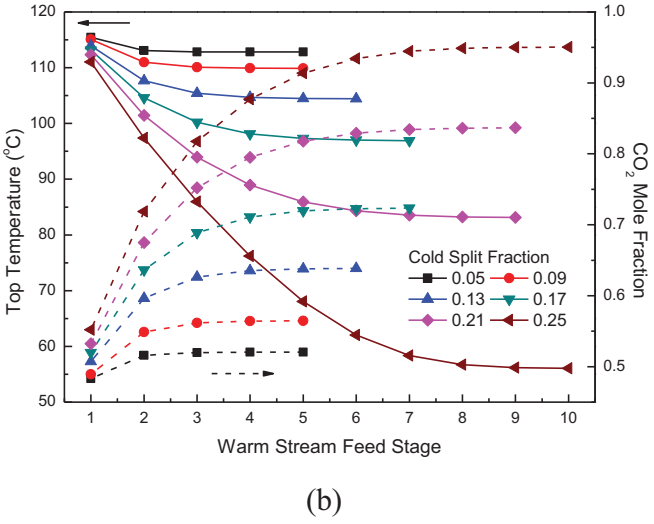

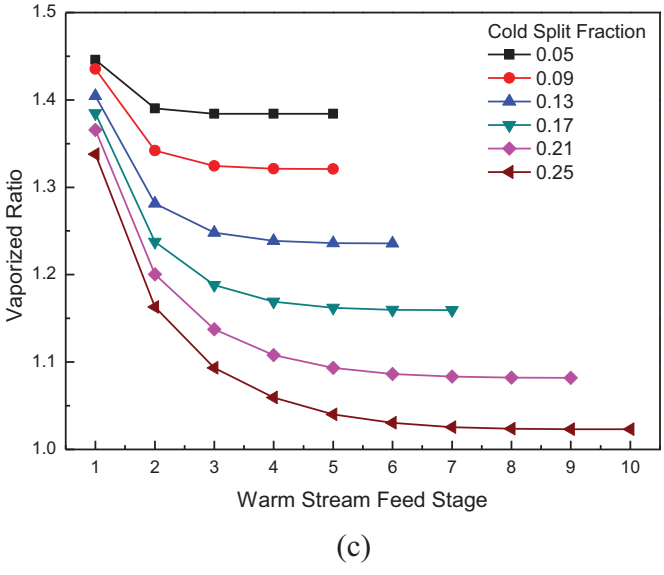

Fig. 6. At CO_2 lean loading of 0.22, where (a) reboiler duty, (b) top temperature (solid lines) and CO_2 purity (dashed lines), and (c) vaporized ratio of overhead flow to the captured CO_2, on varying the warm-rich feed stage.

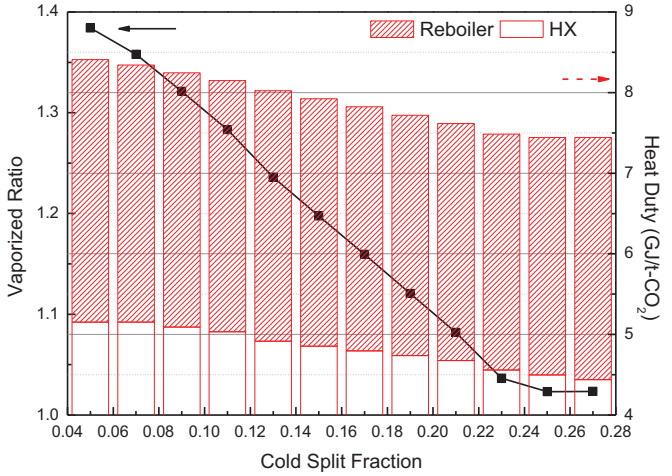

Fig. 7. Overall energy requirement dominated by the vaporized ratio at a CO_2 lean loading of 0.22.

the limiting upper and lower amounts of cold-rich bypass, the recovered and reboiler duties are competitive on varying the cold-split fraction. As shown in Fig. 8, at a CO_2 lean loading of 0.22, the reboiler duty was reduced with an increasing cold-split fraction until the cold-split fraction was above 0.23. Fig. 8 also shows the reboiler duty at CO_2 lean loadings of 0.24 and 0.26 at which the minimum reboiler energy is around 2.91 GJ/t-CO_2 at a lean loading of 0.24 and a cold split fraction of 0.21.

4.2. Interheated stripper

In this study, a single interheater was considered and the stripper pressure was set at 3 atm. The semi-lean solvent was drawn from the tenth stage of the stripper and heated by the IH using a hot lean solvent, which was then returned to the eleventh stage, and the minimum temperature approach of IH was set as 5 °C. Fig. 9(a) compares the reboiler duty of standard and IH processes, in which the required energy consumption is reduced by the IH stripper, and the top temperature of the IH stripper also decreases. Because the partial sensible heat of the hot lean solvent was recovered by the interheater, the temperature of the warm-rich solvent was lower than that of the

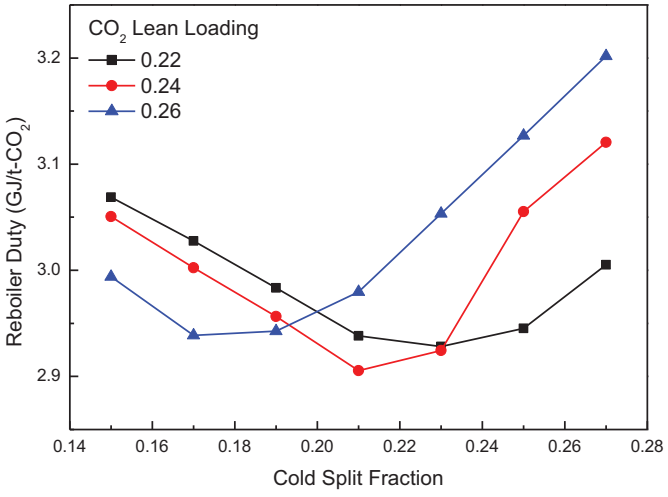

Fig. 8. Comparison of reboiler duty with varying CO_2 lean loadings and cold-split fractions.

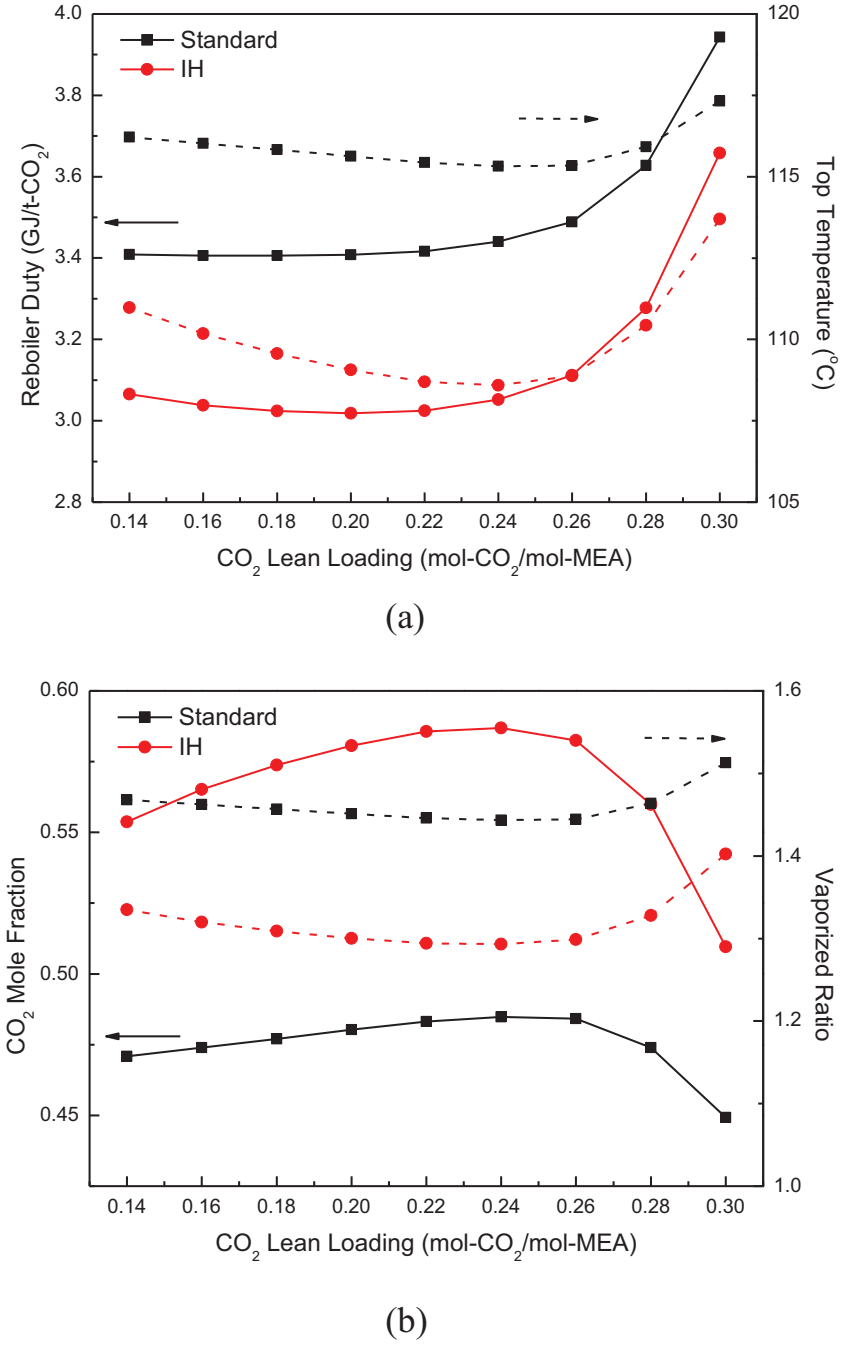

Fig. 9. Comparison of the results of standard and IH processes, where (a) reboiler duty (solid lines) and top temperatures (dashed lines), and (b) CO_2 purity (solid lines) and vaporized ratio (dashed lines).

standard stripper. Fig. 9(b) illustrates that CO_2 purity in the overhead vapor varies with changes to the top temperature and the vaporized ratio of the overhead flow to the captured CO_2 is also affected. The results of Fig. 9 demonstrate that the energy-saving mechanism of the IH stripper is identical to that of the CSB process, due to variations in the vaporized amounts that is dominated by top CO_2 purity.

Fig. 10 is a flow diagram illustrating CSB integrated with the IH stripper in which the semi-lean solvent is drawn from the tenth stage, heated and returned to the next stage. The feed location of the warm-rich solvent is moved downward from the top until the reboiler duty remains unchanged. Fig. 11(a) shows the required energy at a lean loading of 0.20, moving the warm-rich feed stage downward for each cold-split fraction (the dashed line represents the simulation result of a standard stripper). The figure shows that at a constant cold-split fraction the reboiler duty reduces as the warm-rich feed stage moves downward, until the energy consumption remains unchanged. As discussed earlier, the top temperature of the stripper reduces as the warm-rich feed stage moves downwards. The top CO_2 purity increases with lowering of the top temperature; therefore, the vaporized amounts of overhead flow decrease with the dashed lines shown in Fig. 11(b). Fig. 11 shows that the energy reduction achieved using the integrated process is also as a result of the lower amounts of vaporized overhead flow.

Fig. 12 demonstrates that the overall energy requirements of the integrated IH and CSB system at a CO_2 lean loading of 0.20 was affected by the vaporized ratio at the top. In the case of a low cold-split-fraction e.g., less than 0.07, the recovered energy by the IH and HX system remained constant on varying the cold-split fraction. In

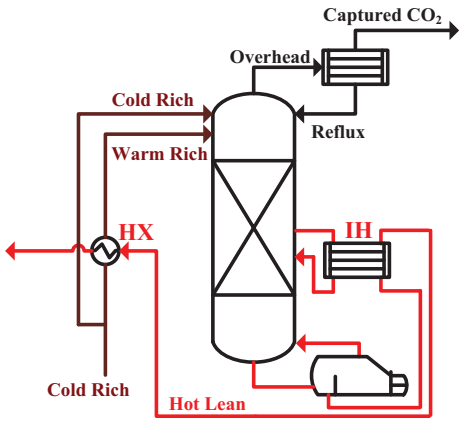

Fig. 10. The process flow diagram integrating CSB with IH.

these cases, the reduction of overall energy was contributed to the reboiler duty, whilst decreasing the vaporized ratio at the top. Once the recovered energy decreases due to the excess amounts of bypass, the deficiency is compensated for by the reboiler duty. As shown in Fig. 13, the reboiler duty decreases as the cold-split fraction increases

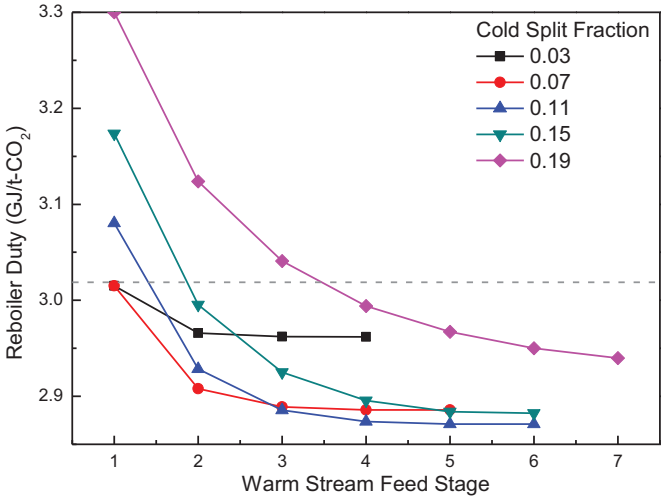

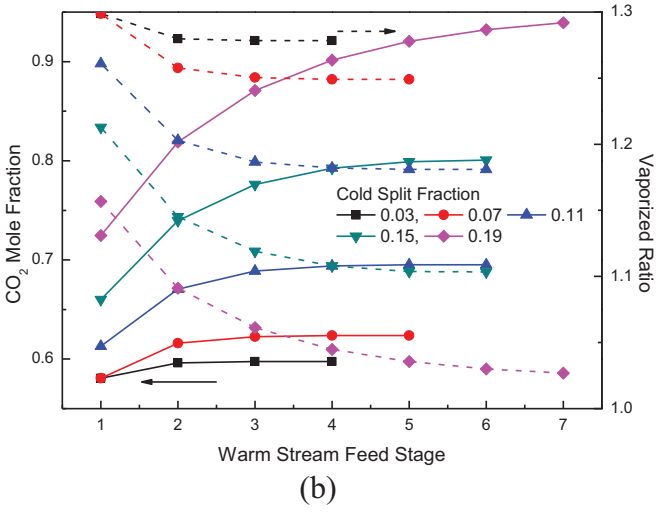

Fig. 11. At a CO_2 lean loading of 0.20, where (a) reboiler duty, and (b) CO_2 mole fraction (solid lines) and vaporized ratio (dashed lines), with varying cold-split fractions and a warm-rich feed stage.

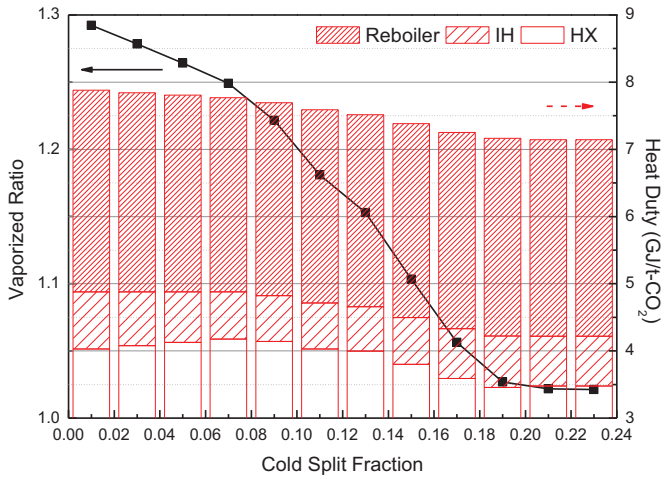

Fig. 12. Overall energy requirement and vaporized ratio (on the top) for the integrated process.

in the first instance; then, the reboiler duty increases as the cold-split fraction becomes larger than the values that are dependent on CO_2 lean loading. Fig. 13 shows that a minimum energy consumption of 2.83 GJ/t-CO_2 can be found at a lean loading value of 0.22 and a cold-split fraction of 0.11.

4.3. Lean vapor compression

As discussed earlier in Section 3, high temperatures in the stripper favor CO_2 desorption from carbamate and bicarbonate that lead to the CO_2 stripper being operated at a high pressure, in general. The lean solvent at the bottom can be flashed to produce a gaseous stream. This can subsequently be compressed and fed back into the bottom of stripper as an additional heat source. Thereby, the reboiler duty can be reduced but the compressor work also needs to be considered when evaluating energy-saving performance. In this study, a thermal efficiency of 35.6% [2] was used to convert the electric power into thermal energy for evaluating the overall energy requirement of LVC and its integrated processes. Fig. 14 compares the required energy for the stripper when operated at 2 atm and the flash drum pressure set at 1 atm. The overall duty consists of the reboiler duty and the thermal energy for the compressor work. The results show that reboiler duty is significantly reduced by the LVC configuration. When combined with the thermal energy of the compressor, the stripper (operated at 2 atm) can achieve

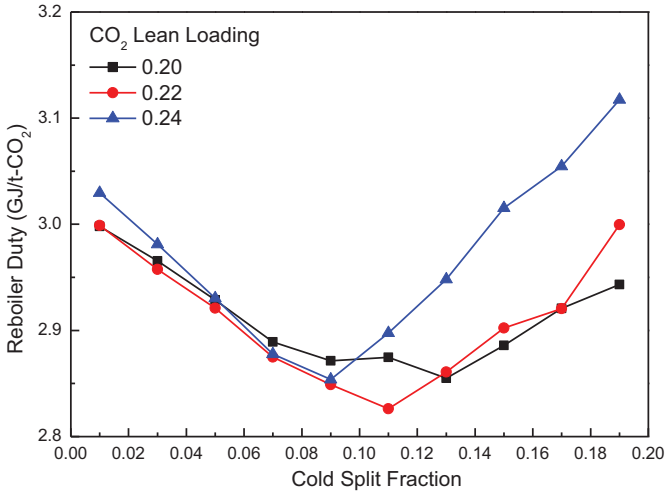

Fig. 13. Comparison of reboiler duty with varying CO_2 lean loadings and cold-split fractions.

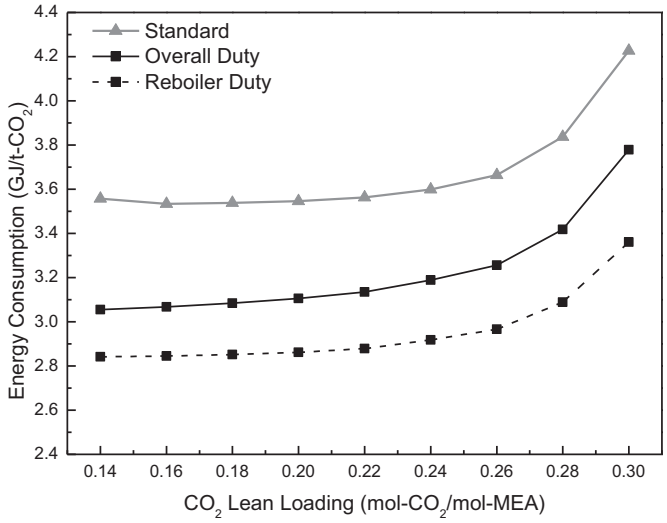

Fig. 14. Comparison of energy consumption by the standard and LVC processes at a stripper pressure of 2 atm.

the minimum overall duty of 3.06 GJ/t-CO_2 at a lean loading of 0.14. Fig. 15 shows the results of the LVC configuration, for a stripper operated at 3 atm, in which the pressure of the flash drum was set as 2 atm and 1 atm, respectively. As shown in Fig. 15(a), at a lean loading of 0.14, the reboiler duty can be reduced from 3.41 to 3.04 GJ/t-CO_2 at 2 atm and 2.48 GJ/t-CO_2 at 1 atm. However, taking the thermal energy of compressor work into account, the overall duty is comparable with the flash drum when operated at 1 atm and 2 atm. Considering the limitation of the reboiler temperature, for which the CO_2 lean loading needs to be larger than or equal to 0.20, as shown in Fig. 4(b), the minimum overall duties were 3.14 and 3.15 GJ/t-CO_2 for the flash drum operated at 2 atm and 1 atm, respectively, and where the CO_2 lean loading was 0.20. Fig. 15(b) compares the top CO_2 purity for the standard and LVC processes, where the stripper pressure was at 3 atm and the flash drum pressure was set as 2 atm and 1 atm, respectively. The solid lines in Fig. 15(b) show that the LVC configuration has a higher CO_2 purity (on the top) because the flashed liquid has a lower temperature than that of the hot lean solvent. This leads to the stripper being fed with a warm-rich solvent at a lower temperature. As discussed earlier in the previous subsections, higher CO_2 purity on the top results in lower vaporized amounts, as shown by the dashed lines in Fig. 15(b). Therefore, the energy-saving mechanism in advanced stripper configurations (LVC, IH and CSB) is identical. The CSB flow, or the warm-rich flow at a lower temperature from the LVC or IH processes, reduces the top temperature of the stripper which in turn increases CO_2 purity in the overhead flow. In the case of a constant CO_2 removal rate, lower amounts of overhead vapor need to be vaporized by the reboiler duty when the CO_2 purity is high in the overhead flow. It is this which provides the energy-saving mechanism for advanced stripper configurations.

Fig. 16 shows the process flow diagram integrating LVC with CSB. Considering the thermal degradation of the MEA solvent, the stripper pressure was simulated at 2 and 3 atm. In the former cases, an adiabatic flash drum was simulated at atmospheric pressure and the flashed gas was compressed back into the stripper, in which an isentropic compressor was applied. When the stripper pressure was simulated at 3 atm, the adiabatic flash drum was simulated at 2 and 1 atm, respectively. As shown in Fig. 14, the stripper operated at 2 atm with LVC seems to be a promising approach, as the thermal degradation of the MEA solvent can be relieved by the lower reboiler temperature, as shown in Fig. 4(b). The results of simulating the stripper at 2 atm and the flash drum at 1 atm are shown in Fig. 17 where the recovered duty by the HX significantly decreased as the cold-split fraction increased. The flashed liquid temperature at 1 atm, which was around 100 °C, was much lower than the hot lean temperature.

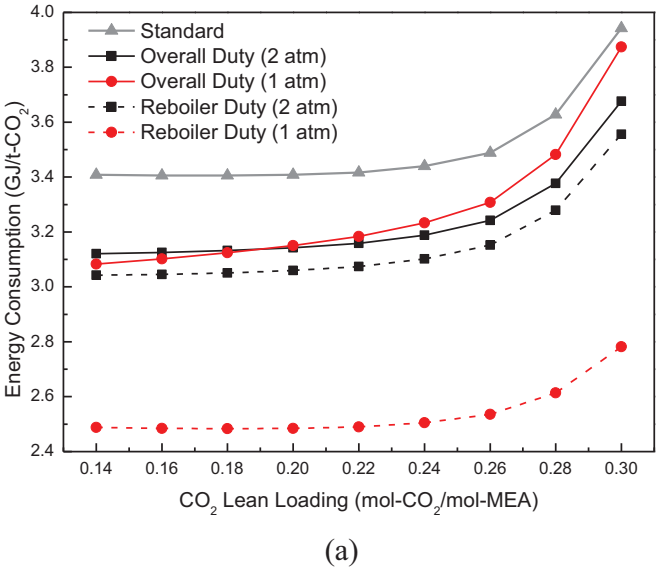

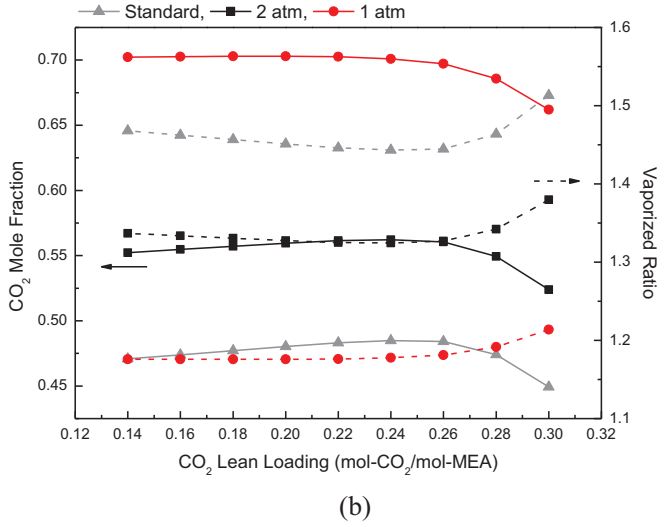

Fig. 15. LVC configuration for a stripper pressure of 3 atm, where (a) the energy consumption of standard and LVC processes, and (b) top CO_2 purity (solid lines) and vaporized ratio (dashed lines).

Heat recovery by the HX process was largely affected by the amounts of warm-rich flow. This is because temperature increases in the warm-rich solvent were limited by the lower temperature of the

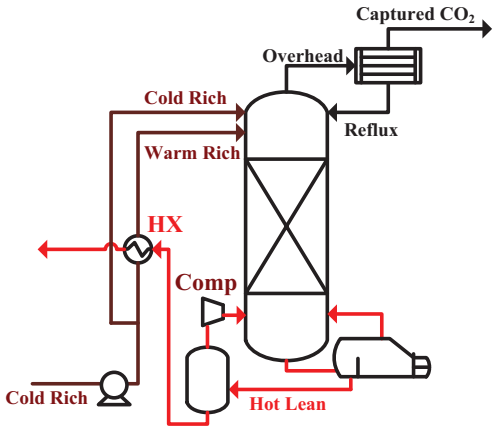

Fig. 16. The process flow diagram integrating CSB with LVC.

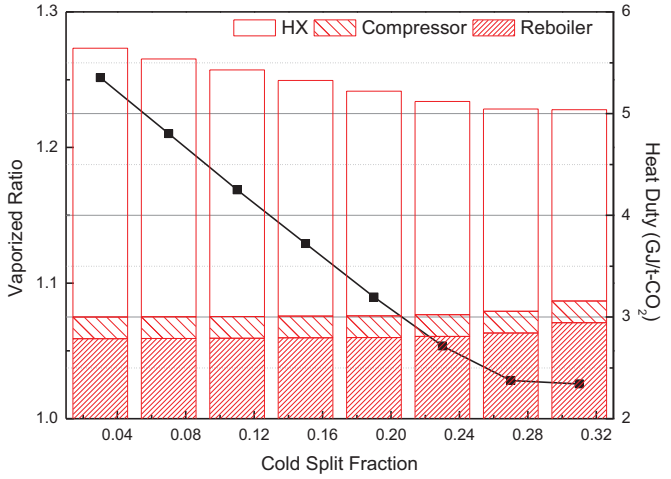

Fig. 17. Stripper pressure at 2 atm and a CO_2 lean loading of 0.14, the overall energy requirement and top vaporized ratio for the integrated process.

flashed liquid. Consequently, the heat recovery dropped lower and lower as the cold-split fraction increased, as shown in Fig. 17. The reboiler duty did not benefit from lowering the vaporized ratio on the top, whilst increasing the cold-split fraction. Similar results could be observed in Fig. 18(a), when the stripper was operated at 3 atm and the flash drum was set at 1 atm. The reduction of vaporized ratio on the top relieves the overall heat duty; however, the energy reduction may not contribute to the reboiler duty due to the poor heat recovery by the HX. To improve the heat recovery performance, the flashed liquid temperature should be increased by raising the flash drum pressure. Comparing Fig. 18(a) and (b), the heat recovery performance was effectively improved by raising the flash drum pressure from 1 atm to 2 atm; in addition, the reduction of reboiler duty can be observed by varying the cold-split fraction. Fig. 19 shows the overall energy requirement, including the reboiler duty and thermal energy for compressor work, with varying cold-split fractions. The minimum energy requirement of 2.78 GJ/t-CO_2 can be found at a CO_2 lean loading of 0.22 and a cold-split fraction of 0.19.

4.4. Summary

The energy-saving mechanism for advanced stripper configurations was investigated in this study. In the review paper, Le Moullec et al. [15] indicated that energy reduction using the CSB process was due to heat recovery from vapor that was directly passed into the condenser. The released vapor can be used to provide stripping heat for the CSB flow. However, in this study the energy-saving stemmed from capturing the same amount of CO_2 as less solvent needs to be vaporized by the reboiler duty if the overhead CO_2 is purer. The energy savings can therefore be fulfilled by reducing the top temperature with the CSB flow. The general energy saving principle for the CSB process is that a low temperature at the top reduces the amount of overhead vapor, which in turn reduces the reboiler duty. The same explanation can be applied to the IH and LVC configurations. The partial sensible heat of the hot lean solvent was recovered by the interheater or reduced by the flash drum at a lower pressure before entering the HX. Thereby, the temperature of the warm-rich solvent was reduced resulting in a lower temperature at the top of the stripper. Table 2 summarizes the simulation results of standard and advanced stripper configurations in which all the top temperatures of the advanced strippers are lower than those of the corresponding standard processes, at the same stripper pressure. Therefore, the reboiler duty can be reduced because a lower amount of vapor is generated. Fig. 20 shows the correlation between CO_2 purity and the top temperature, in which the CO_2 purity can be increased either by increasing the stripper pressure or by reducing the top

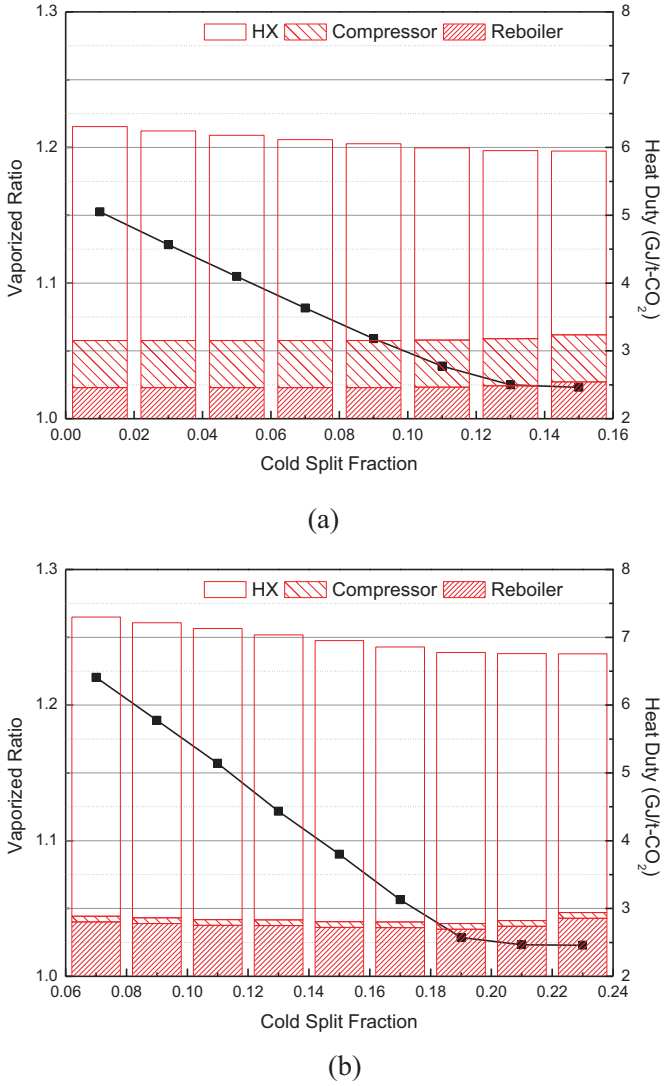

Fig. 18. Overall energy requirement and top vaporized ratio for the integrated process at a CO_2 lean loading of 0.20 and a stripper pressure of 3 atm, with the flash drum maintaining pressures of (a) 1 atm, and (b) 2 atm.

temperature. As listed in Table 2, in the case of a standard stripper, by increasing the operating pressure from 2 atm to 3 atm, the minimum corresponding energy requirement can be reduced from 3.53 to 3.41

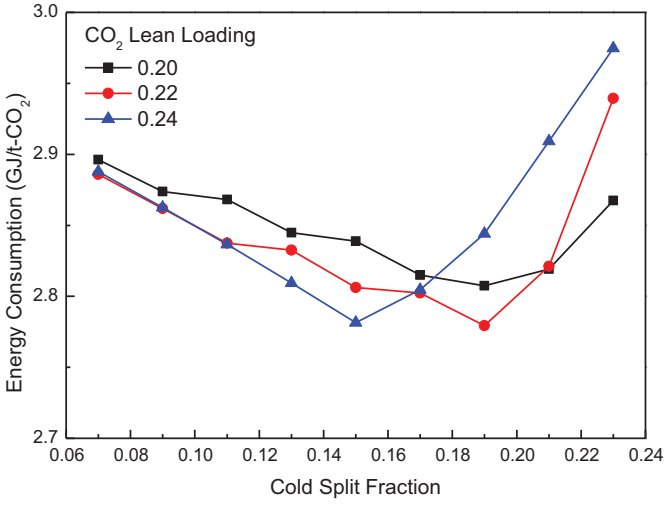

Fig. 19. Energy requirement for the integrated LVC and CSB process.

Table 2
Summary of simulation results for both standard and advanced stripper configurations.

	Standard		CSB	IH		LVC		CSB + IH	CSB + LVC
CO_2 stripper pressure (atm)	2	3	3	3	2	3	3	3	3
Bottom temperature (°C)	123	134	132	134	123	133	134	133	133
Top temperature (°C)	106	116	68	109	97	99	111	99	61
CO_2 mole fraction	0.444	0.480	0.912	0.581	0.594	0.703	0.560	0.704	0.938
Vaporized ratio	1.519	1.451	1.041	1.300	1.283	1.176	1.327	1.173	1.029
Warm-rich feed stage			9					6	9
Cold-split fraction			0.21					0.11	0.19
CO_2 loading of lean solvent	0.16	0.20	0.24	0.20	0.14	0.20	0.20	0.22	0.22
Lean solvent/flue gas	2.89	3.33	3.98	3.33	2.72	3.33	3.33	3.61	3.61
Flash drum (atm)					1	1	2		2
Required energy (GJ/t-CO_2)									
CO_2 stripper	3.53	3.41	2.91	3.02	2.84	2.48	3.06	2.83	2.69
Compressor power [a]					0.21	0.67	0.08		0.08
Overall energy	3.53	3.41	2.91	3.02	3.05	3.15	3.14	2.83	2.78
Energy-saving performance	ref.	3%	18%	14%	14%	11%	11%	20%	21%

[a] Thermal efficiency was assumed as 35.6% (Cottrell et al., 2008).

GJ/t-CO_2, which is a reduction of around 3%. Additionally, in a standard stripper, high temperatures encourage CO_2 to be desorbed from the carbamate and bicarbonate that enrich the CO_2 purity from 0.444 to 0.480. It also reduces the vaporized ratio at the top from 1.519 to 1.451 and so the reboiler duty can be reduced slightly.

Fig. 20 illustrates that the advanced stripper configurations share the same correlations at a constant stripper pressure. The figure also shows that the IH and LVC configurations were not efficient at increasing the top CO_2 purity, in comparison with the CSB process and its combinations. This suggests that the energy-saving performances of CSB and its combinations exceed those of the IH and LVC configurations. As listed in Table 2, the CSB configuration can reduce required energy by 18% in comparison with the reference process (a standard stripper at 2 atm). On the other hand, the IH and LVC processes lower energy consumption by 14% and 11–14%, respectively. The major energy reduction for advanced configurations is attributed to decreasing the vaporized ratio of overhead vapor to captured CO_2. The CSB configuration reduces the vaporized ratio from the baseline of 1.519 to 1.041 and the IH and LVC processes reduce the vaporized ratio to 1.300 and 1.176–1.327, respectively, as listed in Table 2. Energy reductions of 20% and 21% are achieved by integrating CSB with IH or LVC, respectively. The improvement in energy savings is only 2% to 3%, which compares with the reduction achieved using the CSB process by implementing either an additional interheater or a flash drum and compressor set. The improvement is not as promising as the review paper [15] declared. A possible explanation for this could be that the energy-saving performance by the CSB configuration was underestimated. Most literature noted that the cold-split fraction may determine the minimum energy consumption. However, it was perhaps overlooked that the feed location for the warm-rich solvent also affects the energy-saving performance.

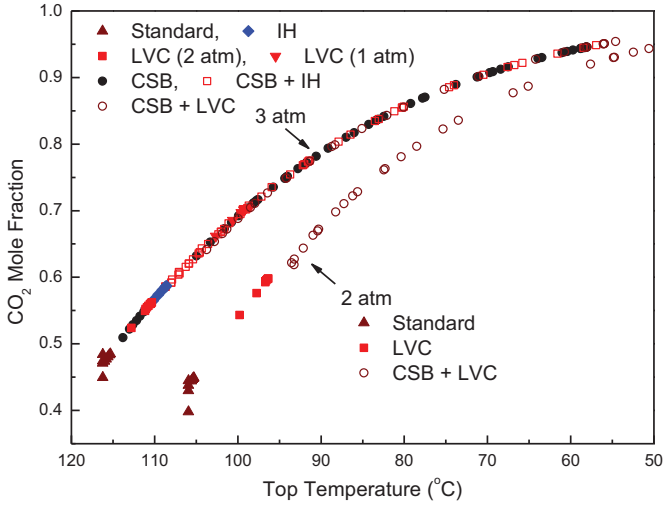

Fig. 20. Correlation between the top temperature and CO_2 purity for both standard and advanced stripper configurations.

5. Conclusion

The energy-saving mechanism of advanced stripper configurations including CSB, IH, and LVC, was investigated in this study. In the literature [14,15], the CSB modification was recognized for recovering vapor heat from the overhead flow that was fed directly into the condenser. The interheater was used to adjust the temperature profile of the stripper by raising the temperature of the bottom section that favors CO_2 desorption reactions [16]. Combining the CSB and IH configurations was proposed to optimize on their respective advantages and enhance energy-saving. However, as the energy-saving mechanism of the above-mentioned modifications is identical, it may have been optimistic to assume an enhanced energy-saving performance.

With a constant CO_2 removal rate and a higher CO_2 purity at the top of the stripper, less overhead vapor needs to be generated. The reduction in vaporization requirements was found to be the general energy-saving mechanism for both the pressurized standard stripper and the advanced stripper configurations. Although the high temperature of the pressurized stripper favors CO_2 desorption, thermal degradation of the MEA solvent accelerates as the reboiler temperature is above 135 °C. On the other hand, reducing the top temperature of the stripper to enhance CO_2 purity is the general principle behind advanced stripper configurations. A high CO_2 purity in the overhead flow can effectively reduce the amounts of overhead vapor to be generated, which is composite of heat recovered by the HX, reboiler duty and compressor work (if the LVC was applied). When the reduced energy, due to the lower amounts of vapor, is contributed to poor heat recovery, the energy-saving design may not be fulfilled. Therefore, maintaining a reliable heat recovery, whilst reducing the amounts of vapor to be generated, is the general energy-saving design principle for advanced stripper configurations.

Declaration of Competing Interest

The authors declare that they have no known competing financial interests or personal relationships that could have appeared to influence the work reported in this paper.

Acknowledgment

This work was supported by the Ministry of Science and Technology, Republic of China, under Grant 107-2221-E-029-023.

References

[1] Rochelle GT. Amine scrubbing for CO_2 capture. Science 2009;325:1652–4.
[2] Cottrell AJ, McGregor JM, Jansen J, Artanto Y, Dave N, Morgan S, Pearson P, Attalla MI, Wardhaugh L, Yu H, Allport A, Feron PHM. Post-combustion capture R&D and pilot plant operation in Australia. Energy Proc 2008;1:1003–10.
[3] Mathonat C, Majer V, Mather AE, Grolier JPE. Use of flow calorimetry for determining enthalpies of absorption and the solubility of CO_2 in aqueous monoethanolamine solutions. Ind Eng Chem Res 1998;37:4136–41.
[4] Kim I, Svendsen HF. Heat of absorption of carbon dioxide (CO_2) in monoethanolamine (MEA) and 2-(aminoethyl) ethanolamine (AEEA) solutions. Ind Eng Chem Res 2007;46:5803–9.
[5] Notz R, Mangalapally HP, Hasse H. Post combustion CO_2 capture by reactive absorption: pilot plant description and results of systematic studies with MEA. Int J Greenh Gas Control 2012;6:84–112.
[6] Mangalapally HP, Hasse H. Pilot plant study of post-combustion carbon dioxide capture by reactive absorption: methodology, comparison of different structured packings, and comprehensive results for monoethanolamine. Chem Eng Res Des 2011;89:1216–28.
[7] Dugas RE. Pilot plant study of carbon dioxide capture by aqueous monoethanolamine Master thesis, Chemical Engineering. University of Texas at Austin; 2006.
[8] Zhang Y, Chen H, Chen CC, Plaza JM, Dugas R, Rochelle GT. Rate-based process modeling study of CO_2 capture with aqueous monoethanolamine solution. Ind Eng Chem Res 2009;48:9233–46.
[9] Onda K, Takeuchi H, Okumuto Y. Mass transfer coefficients between gas and liquid phases in packed columns. J Chem Eng Jpn 1968;1:56–62.
[10] Stichlmair J, Bravo JL, Fair JR. General model for prediction of pressure drop and capacity of countercurrent gas/liquid packed columns. Gas Sep Purif 1989;3:19–28.
[11] Fair JR, Bravo JL. Prediction of mass transfer efficiencies and pressure drop for structured tower packings in vapor/liquid service. Inst Chem Eng Symp Ser 1985 Jul: 183–200.
[12] Bravo JL, Rocha JA, Fair JR. A comprehensive model for the performance of columns containing structured packings. Inst Chem Eng Symp Ser 1992;129:439–57.
[13] Aboudheir A. Kinetics, modeling and simulation of CO_2 absorption into highly concentrated and loaded MEA solutions Ph.D. thesis, Chemical Engineering. University of Regina; 2002.
[14] Lin YJ, Madan T, Rochelle GT. Regeneration with rich bypass of aqueous piperazine and monoethanolamine for CO_2 capture. Ind Eng Chem Res 2014;53:4067–74.
[15] Le Moullec Y, Neveux T, Azki AA, Chikukwa A, Hoff KA. Process modifications for solvent-based post-combustion CO_2 capture. Int J Greenh Gas Control 2014;31:96–112.
[16] Karimi M, Hillestad M, Svendsen HF. Positive and negative effects on energy consumption by interheating of stripper in CO_2 capture plant. Energy Proc 2012;23:15–22.
[17] Higgins SJ, Liu YA. CO capture modeling, energy savings, and heat pump integration. Ind Eng Chem Res 2015;54:2526–53.
[18] Ahn H, Luberti M, Liu Z, Brandani S. Process configuration studies of the amine capture process for coal-fired power plants. Int J Greenh Gas Control 2013;16:29–40.
[19] Aspen Technology. Rate-based model of the CO2 capture process by MEA using ASPEN plus. 2017.
[20] Davis J, Rochelle GT. Thermal degradation of monoethanolamine at stripper conditions. Energy Proc 2009;1:327–33.